PHYSICAL REVIEW E VOLUME 61, NUMBER 3 MARCH 2000

Ordering of viscous liquid mixtures under a steady shear flow

Zhenyu Shou and Amitabha Chakrabarti
Department of Physics, Cardwell Hall, Kansas State University, Manhattan, Kansas 66506-2601
(Received 10 May 1999)

Through extensive numerical simulations, we study phase separation in quenched viscous liquid mixtures under an external shear flow. Formation of a layered structure in steady state normal to the shear direction is shown to develop in the strong shear limit. The characteristic width of the layered domains follows a power law as a function of the shear rate, with a power-law exponent in agreement with experimental results. Shear-induced rheological behavior of the mixture is also examined in terms of the excess viscosity. Observed power-law behavior of the maximum excess viscosity, which occurs at an intermediate time, agrees quite well with theoretical scaling predictions.

PACS number(s): 64.60.Cn, 61.41.+e, 64.60.My, 64.75.+g

Despite extensive recent effort [1], ordering of quenched liquid mixtures under a shear flow is not fully understood yet. When spinodal decomposition of a liquid mixture takes place in the presence of an externally applied shear flow, a strikingly elongated domain structure and peculiar rheological effects can result. These phenomena have recently been observed in experiments with various viscous liquid mixtures [2,3] such as low molecular weight polymer blends and pseudobinary mixtures of two different polymers in a common solvent. Linear stability analysis [4] suggests that shear flow indeed stabilizes such cylindrical domains against various instabilities. The formation of highly anisotropic domains has also been explained [3] as a repeated breakup of spherical droplets in a strong shear flow. There is, however, no theoretical explanation for the observed power-law behavior [2] shown by the thickness of these layered domains as a function of the shear flow rate. Shear-induced rheological behavior of phase separating liquid mixtures is also intriguing. The breakup of domains elongated by shear leads to an excess viscosity $\Delta\eta$. This quantity shows a maximum at some *intermediate time* t_m, and then relaxes to much smaller values at late times. $(\Delta\eta)_{\max}$ scales with shear rate as well, but the situation is not clear as different theoretical calculations [5,6] and experimental measurements [7] for the power-law exponent do not seem to agree with each other.

In this Rapid Communication, we address both these issues of shear-induced morphology of phase separated domains and the rheological behavior of the liquid mixture by carrying out a detailed simulation of domain growth in two dimensions. The model considered by us incorporates hydrodynamic interactions and an externally applied steady shear flow. Many previous simulations [5] typically did not include any hydrodynamic interactions in the model calculations. In limited cases, where hydrodynamics was included (in a coarse-grained model [8] or in a molecular dynamics simulation [9]), the simulations were not carried out to late times. As a result, layered domains were not observed in these simulations. In the present study, we not only observe this extreme anisotropic phase but also characterize it by computing the domain size in steady state for many different strengths of the shear flow rate. The scaling of the domain size with the shear flow rate found in our simulations is in good agreement with experimental observations. In addition, scaling of the excess viscosity as a function of the shear flow rate found in simulations agrees quite well with scaling predictions.

We start from a model-*H* formulation [10] of a quenched liquid mixture described by a Landau-Ginzburg type free-energy functional F. In this formulation the order parameter ϕ and the velocity field $\mathbf{u}$ satisfy the following set of equations:

$$\frac{\partial\phi}{\partial t}+\mathbf{u}\cdot\boldsymbol{\nabla}\phi=M\cdot\nabla^2\frac{\delta F}{\delta\phi}+\zeta, \tag{1}$$

$$\rho\left(\frac{\partial\mathbf{u}}{\partial t}+\mathbf{u}\cdot\boldsymbol{\nabla}\mathbf{u}\right)=\eta\nabla^2\mathbf{u}-\phi\boldsymbol{\nabla}\frac{\delta F}{\Delta\phi}-\boldsymbol{\nabla}P+\theta, \tag{2}$$

along with the incompressibility condition, $\boldsymbol{\nabla}\cdot\mathbf{u}=0$. Here, Eq. (1) is a modified Cahn-Hilliard equation and Eq. (2) is a modified Navier-Stokes equation. ζ and θ are the thermal noise terms. Since the fluid is highly viscous, the inertial terms in the Navier-Stokes equation can be neglected. Under such an overdamped relaxation approximation, and a suitable rescaling of the order-parameter, the velocity field, and space and time, the governing equations can be rewritten as

$$\frac{\partial\phi}{\partial t}+\mathbf{u}\cdot\boldsymbol{\nabla}\phi=\nabla^2(-\phi+\phi^3-\nabla^2\phi)+\xi, \tag{3}$$

$$\nabla^2\mathbf{u}=C\phi\boldsymbol{\nabla}(-\phi+\phi^3-\nabla^2\phi)+\boldsymbol{\nabla}P+\theta, \tag{4}$$

along with the usual incompressibility condition. Here C is a constant which is inversely proportional to the viscosity η. In the presence of an externally applied steady shear flow in the $\hat{\mathbf{x}}$ direction, the velocity field can be written as

$$\mathbf{u}(\mathbf{r})=\dot{\gamma}y\hat{\mathbf{x}}+\mathbf{v}(\mathbf{r}), \tag{5}$$

where $\dot{\gamma}$ is the shear rate and $\mathbf{v}(\mathbf{r})$ is the fluctuation part of the velocity field.

Numerical solutions of the above set of equations is computationally demanding, particularly when one needs statistically accurate data for several values of the shear rate. For this reason, our simulations have been restricted to a two-dimensional grid of sizes 128×128 and 256×256 and the

thermal noise terms are not included in the integration. The absence of thermal noise would limit our conclusions to a deep quench case. The order parameter equation is integrated by a straightforward Euler method, while the velocity equations are integrated by using a fast Fourier transform method [11,12]. The sheared boundary condition associated with the original equation is converted to an ordinary periodic boundary condition by the following moving lattice transformation:

$$x' = x - \dot{\gamma} t y, \quad y' = y. \tag{6}$$

The resulting equations after such a transformation become stiff differential equations and numerical instability becomes a serious problem at late times. A remeshing procedure [13] is employed to resolve this problem. The remeshing procedure utilizes the ordinary periodic boundary condition in the flow direction to move data from the skewed lattice points onto a regular square lattice system. After remeshing, the grid progresses from its initial orthogonal position and eventually becomes skewed again when remeshing becomes necessary again [14]. For our square system ($L \times L$), remeshing is done at every integer value of $\dot{\gamma} t$. After this remeshing the integration remains stable in effect for all times when a small enough time-step ($\Delta t = 0.01$) is used.

We consider a critical quench case and compute the pair correlation function in both the x and y directions. The domain size along the x and y directions are computed from the respective pair-correlation functions as the location of the first zero crossing. We have also computed the normalized excess shear viscosity which represents the viscoelastic properties of the mixture. This quantity is related to the off-diagonal average excess shear stress and can be computed as

$$\Delta \eta = -\frac{C}{\dot{\gamma}} \left\langle \frac{\partial \phi}{\partial x} \frac{\partial \phi}{\partial y} \right\rangle. \tag{7}$$

All of these quantities are averaged over at least 20 realizations of the initial condition.

In Figs. 1 and 2 we display typical snapshots [15] of the concentration profile of the system at various times after the quench for two different values of the (rescaled) shear rate $\dot{\gamma} = 0.02$ and 0.05. For early times (i.e., for $\dot{\gamma} t \leqslant 1$), the phase separated domains are isotropic, as the shear effects are yet to perturb their shape. Subsequently, the domains become elongated under the influence of the shear flow. The rupture and recombination of domains become most prominent at intermediate times ($\dot{\gamma} t \gtrsim 1$) and this leads to a maximum in the excess shear viscosity around this time. Finally, at very late times ($\dot{\gamma} t \gg 1$) lamellaelike domains form with a normal along the shear gradient ($\hat{\mathbf{y}}$) direction. The final shape of the domains does not change any further and the system reaches a steady state. Note that the thickness of the lamellae (R_y) at the steady state is much smaller for the larger shear rate.

In order to test a possible scaling relation between the domain size R_y and the shear rate $\dot{\gamma}$, we have carried out the simulation for a large number of shear rates. We observe that as long as the shear rate is larger than a critical value ($\dot{\gamma}_c \approx 0.001$), lamellaelike structures form in the steady state. In Fig. 3 we show a log-log plot of R_y versus $\dot{\gamma}$. The data [16] for all these shear rates fall on a straight line indicating that

$$R_y \sim \dot{\gamma}^{-n}, \tag{8}$$

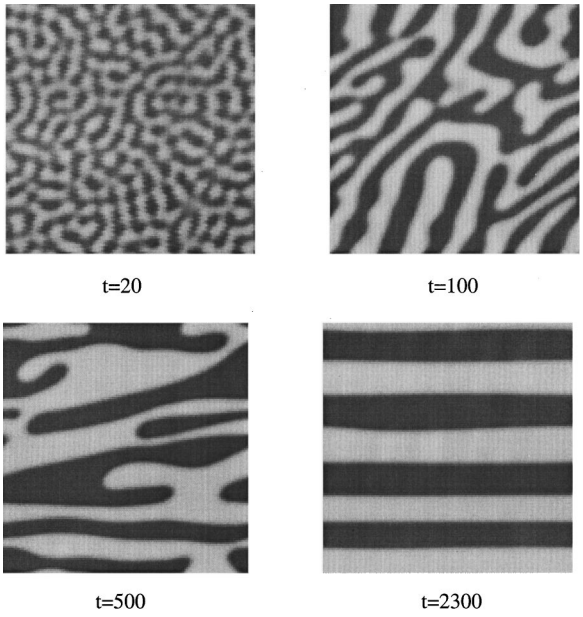

FIG. 1. Typical snapshots of the concentration profile for a shear rate of $\dot{\gamma} = 0.02$. At early times, domains are isotropic. Subsequently, domains become elongated along the flow direction. At late times, lamellar layers normal to the shear flow direction is formed.

with the exponent $n = 0.35 \pm 0.03$, in excellent agreement with the experimental observations of Hashimoto *et al.* [2] To obtain further insight into this scaling law, we *turned off* hydrodynamic interactions and conducted a simulation by solving only the order parameter equation in the presence of a steady shear flow. A similar scaling law is found in this case as well [17] but the exponent n in the absence of hydrodynamics is smaller, $n = 0.22 \pm 0.03$.

A detailed understanding of this scaling law needs a com-

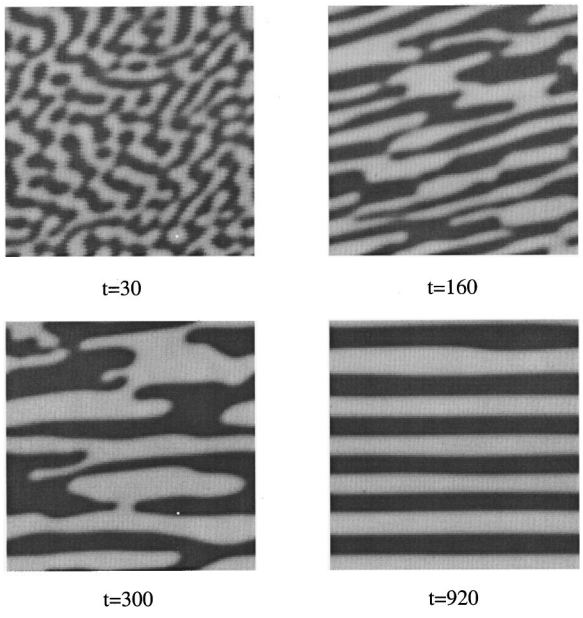

FIG. 2. Same as in Fig. 1 except $\dot{\gamma} = 0.05$ here. Note that the time scales for the formation of anisotropic domains are different in this case. Moreover, the width of the lamellar domains formed at very late times are smaller in this case when compared to Fig. 1.

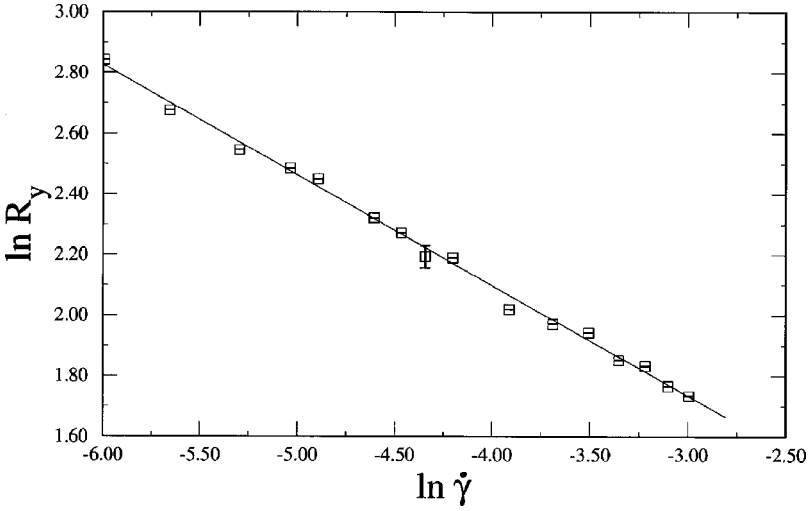

FIG. 3. Log-log plot for the domain size R_y in the steady state vs the shear rate $\dot{\gamma}$ in the presence of hydrodynamics for the critical quench case. A typical error bar is shown for guidance. The slope of the straight line is -0.35.

plete treatment of the shear-induced pattern formation that is not yet available in the literature. However, the following argument, based on a mode-coupling theory by Kawasaki [18], will help shed some light onto the phenomenon. The main new feature of domain growth in the presence of a shear flow is the suppression of the domain fluctuation. The flow field tends to stretch the domains and in the process enlarges the interfacial area, while the interfacial tension tends to minimize it. Since the system eventually reaches a steady state controlled by a balance between the external shear and the intrinsic thermodynamic mechanism, it is reasonable to assume that the relaxation rate of the concentration fluctuation Γ_{qc} should be balanced by the external shear rate $\dot{\gamma}$ as $\Gamma_{qc} \equiv \Gamma(q_c) \sim \dot{\gamma}$. Modes with wave numbers bigger than q_c will have faster relaxation rates, and in consequence will disappear quickly. A small value of q_c would then correspond to a weak shear case, because not many wave numbers $q < q_c$ are affected by the shear. In contrary, a large value of q_c corresponds to a strong shear case as more modes are affected and suppressed by the shear. One can relate the magnitude of q_c to the inverse of some thermal fluctuation correlation length ξ. The relaxation rate of the order parameter fluctuation can be divided into two parts [19,20]. $\Gamma(q) = \Gamma_{\text{hydro}}(q) + \Gamma_{\text{inter}}(q)$, where $\Gamma_{\text{hydro}}(q)$ is associated with the hydrodynamic interactions and has the following form:

$$\Gamma_{\text{hydro}}(q) = \frac{kT}{6\pi n \xi^3} \begin{cases} (q\xi)^2 & \text{for } q\xi < 1 \\ \dfrac{3\pi}{8}(q\xi)^3 & \text{for } q\xi > 1 \end{cases}. \tag{9}$$

$\Gamma_{\text{inter}}(q)$ originates from the contribution of the interface diffusion, and is given by $\Gamma_{\text{inter}}(q) \sim q^2(1+q^2\xi^2)$. For strong shear cases, this yields $\Gamma_{\text{inter}}(q) \sim q^4\xi^2$. Of special interest in this paper is the strong shear limit $q\xi > 1$ where, at a late time regime, the typical size R_y is associated with q_c^{-1} rather than ξ (ξ now will be a small constant representing the width of the interfacial thickness). So, if hydrodynamic effects dominate,

$$R_y \sim q_c^{-1} \sim \dot{\gamma}^{-1/3}, \tag{10}$$

in excellent agreement with experimental measurements. In the absence of hydrodynamic interactions, interfacial diffusion remains the only mechanism to balance shear effects. Consequently, in the strong shear case,

$$R_y \sim q_c^{-1} \sim \dot{\gamma}^{-1/4}. \tag{11}$$

Although the above scaling arguments are limited to three-dimensional systems, the values of the exponent n, both in the presence and absence of hydrodynamics, are in good

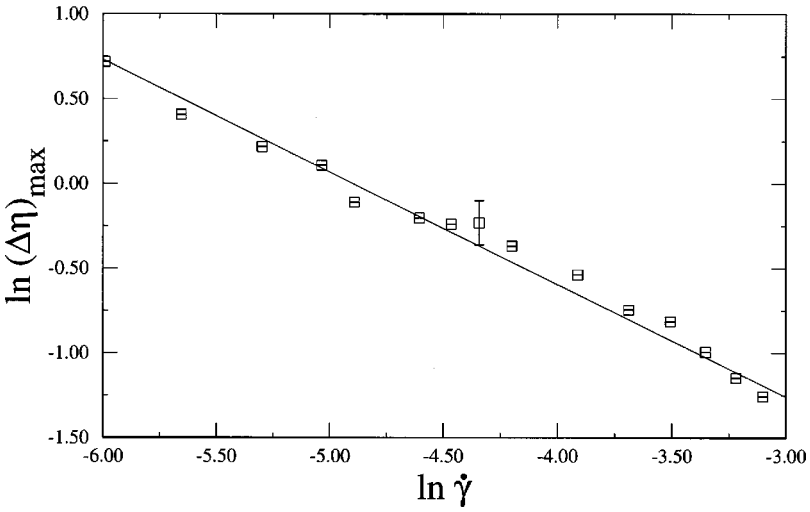

FIG. 4. Log-log plot for the maximum excess viscosity $(\Delta\eta)_{\text{max}}$ vs the shear rate $\dot{\gamma}$. A typical error bar is shown for guidance. The slope of the straight line is -0.65.

agreement with our simulation results for two-dimensional systems. Similar striped structures under strong shear and the same scaling law for the domain size have also been observed in a recent molecular dynamics simulation in two dimensions [21]. Simulations thus suggest that these exponents are similar for both two- and three-dimensional systems.

Next we turn to the scaling of the excess viscosity $\Delta\eta$ as a function of the shear rate. After the system is quenched below the critical point, the excess viscosity increases with time, reaches a maximum value at some intermediate time, and finally decreases gradually to the steady state value. The location of the peak in $\Delta\eta$ corresponds to $\dot{\gamma}t_m \approx 3.5$, in agreement with previous simulations and experiments [5–8]. Observation of the concentration profile clearly indicates that the time t_m of the peak position in $\Delta\eta$ corresponds to the interfacial energy release due to the bursting and coalescing of elongated domains. The maximum excess viscosity $(\Delta\eta)_{\max}$ is expected to scale with the shear rate as

$$(\Delta\eta)_{\max} \sim \dot{\gamma}^{-\nu}. \tag{12}$$

Scaling arguments [5] suggest that $\nu = \frac{2}{3}$, while a recent theoretical calculation [6] in the large-N limit for the order-parameter components and in the absence of hydrodynamics yields $\nu = \frac{1}{2}$. Our results for the excess viscosity are shown in Fig. 4 as a log-log plot. Although there is some scatter in the data even after averaging over a large number of runs, our results are certainly consistent with the scaling result of $\nu = \frac{2}{3}$, but not with the large-N result.

In conclusion, we have carried out a detailed simulation of phase separation in a highly viscous liquid mixture driven by an external steady shear flow. The formation of a layered structure in steady state normal to the shear direction is clearly demonstrated in the simulation in the strong shear limit. The characteristic width of the layered domains follows a power law as a function of the shear rate, in agreement with experimental results. The excess viscosity also shows a power-law behavior in agreement with scaling predictions.

We thank Erik Hobbie, Rodney Fox, and Amalie Frischknecht for many useful discussions. This work has been supported by the Kansas Program for Complex Fluid Flow (Contract No. NSF-EPSCoR) and by the National Science Foundation Grant No. CDA-9724289.

[1] For a review, see A. Onuki, J. Phys.: Condens. Matter **9**, 6119 (1997).
[2] T. Hashimoto, K. Matsuzaka, E. Moses, and A. Onuki, Phys. Rev. Lett. **74**, 126 (1995).
[3] E. K. Hobbie, S. Kim, and C. C. Han, Phys. Rev. E **54**, R5909 (1996).
[4] A. Frischknecht, Phys. Rev. E **56**, 6970 (1997); **58**, 3495 (1998).
[5] T. Ohta, H. Nozaki, and M. Doi, Phys. Lett. A **145**, 304 (1990); J. Chem. Phys. **93**, 2664 (1990).
[6] F. Corberi, G. Gonnella, and A. Lamura, Phys. Rev. Lett. **81**, 3852 (1998).
[7] J. Läuger, C. Laubner, and W. Gronski, Phys. Rev. Lett. **75**, 3576 (1995).
[8] Y. Wu, H. Skrdla, T. Lookman, and S. Chen, Physica A **239**, 428 (1997).
[9] P. Padilla and S. Toxvaerd, J. Chem. Phys. **106**, 2342 (1997).
[10] P. C. Hohenberg and B. I. Halperin, Rev. Mod. Phys. **49**, 435 (1977).
[11] A. J. Bray, Adv. Phys. **43**, 357 (1994).
[12] W. H. Press, B. P. Flannery, S. A. Teulolsky, and W. Vetterling, *Numerical Recipes* (Cambridge University Press, Cambridge, England, 1986).
[13] M. M. Rogers, P. Moin, and W. C. Reynolds, NASA Report No. NCC-2-5 TF-25, 1986 (unpublished).
[14] Even though the remeshing may cause an aliasing error for turbulent systems, it works well in our case.
[15] The snapshots shown here are for a 128^2 system; however, several runs for a larger system of size 256^2 are carried out to make sure that finite-size effects have not influenced results for the exponents.
[16] The domain size R_y computed from the correlation function relates to the ''radius'' of the domains so that its computed value is approximately half of the pattern ''diameter'' shown in the snapshots.
[17] The absolute value of the domain size in the presence of hydrodynamics is also bigger than the domain size in the absence of the hydrodynamics.
[18] K. Kawasaki, Ann. Phys. (N.Y.) **61**, 1 (1970).
[19] T. Hashimoto, T. Takebe, and S. Suehiro, J. Chem. Phys. **88**, 5874 (1988).
[20] M. Doi and T. Ohta, J. Chem. Phys. **95**, 1242 (1991).
[21] R. Yamamoto and X. C. Zeng, Phys. Rev. E **59**, 3223 (1999).